NANO LETTERS

2008
Vol. 8, No. 3
957-961

Layered $Li_{0.88}[Li_{0.18}Co_{0.33}Mn_{0.49}]O_2$ Nanowires for Fast and High Capacity Li-Ion Storage Material

Yoojung Lee,[†,||] Min Gyu Kim,[‡] and Jaephil Cho*[,†,||]

Department of Applied Chemistry, Kumoh National Institute of Technology, Gumi, Korea 730-701, Beamline Research Division, Pohang Accelerator Laboratory, Pohang, Korea 790-784

Received December 3, 2007

ABSTRACT

Layered $Li_{0.88}[Li_{0.18}Co_{0.33}Mn_{0.49}]O_2$ nanowires are prepared using $Co_{0.4}Mn_{0.6}O_2$ nanowires and lithium nitrate as precursors at 200 °C via a hydrothermal method for fast and high capacity Li-ion storage material. The obtained nanowires exhibit a reversible capacity of 230 mAh/g between 2 and 4.8 V, even at the high current rate of 3600 mA/g.

One-dimensional nanostructured materials have been intensively investigated for possible applications related to their magnetic properties and optical properties.[1–4] The superior characteristics of these materials over bulk counterparts originate mainly from their limited crystal dimensions with a very high surface-to-bulk ratio. For electrode materials in lithium batteries, such a high surface area can provide higher electrode/electrolyte contact areas, which can lead to shorter diffusion paths with the particles and more facile intercalation for Li ions. In addition, the reduced strain of intercalation and contributions from charge storage at the surface can also contribute to the Li capacity, compared with bulk counterparts. In this regard, TiO_2 and SnO_2 nanotubes, nanowires and rods have been investigated thoroughly for possible applications as anode materials.[5–14] However, a direct synthetic method for obtaining 1D $LiMO_2$ cathode (M = transition metals) nanowires has not been reported. An alternative method that utilizes the chemical oxidation of pristine bulk $LiMn_{0.5}Ni_{0.5}O_2$ powders was reported by Park et al. The obtained nanowires were lithium- and Ni-deficient $Li_xMn_{0.67}Ni_{0.33}O_2$.[15] The reversible capacity of these nanowires was ~160 mAh/g between 4.8 and 2 V at a current density of 20 mA/g.

Recently, Mn-rich lithium metal oxides such as $Li[Li_{1/3-2x/3}Mn_{2/3-x/3}M_x]O_2$ cathodes are currently receiving significant interest as cathode materials for Li-ion batteries. These materials can provide capacities greater than 200 mAh/g if initially charged to 4.5 V or higher.[16–24] In spite of the capacity advantage, a rapid capacity fade occurs at higher C rates; for instance, over 50% capacity fade was observed when the current was increased from 20 to 200 mA/g in $Li[Ni_{0.2}Li_{0.2}Mn_{0.6}]O_2$.[24] However, Cho et al. recently reported that $Li[Ni_{0.41}Li_{0.08}Mn_{0.51}]O_2$ nanoplates exhibited greatly improved rate capabilities at a 3C rate compared with a bulk counterpart prepared via a coprecipitation method.[25]

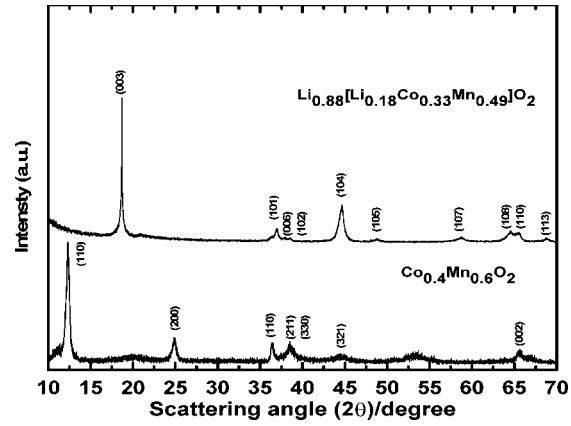

Figure 1. Powdery XRD patterns of $Co_{0.4}Mn_{0.6}O_2$ and $Li_{0.88}[Li_{0.18}Co_{0.33}Mn_{0.49}]O_2$ nanowires.

In this study, the direct synthesis of layered $Li_{0.88}[Li_{0.18}Co_{0.33}Mn_{0.49}]O_2$ nanowires is demonstrated using nanowire $Co_{0.4}Mn_{0.6}O_2$ and lithium nitrate as precursors at 200 °C via a hydrothermal method for high capacity of Li-ion storage material. The obtained nanowires exhibit a reversible capacity of 230 mAh/g between 2 and 4.8 V, even at the high rate of 3600 mA/g.

* Corresponding author. E-mail: jpcho@hanyang.ac.kr.
[†] Department of Applied Chemistry, Kumoh National Institute of Technology.
[‡] Beamline Research Division, Pohang Accelerator Laboratory.
[||] Current address: Department of Applied Chemistry, Hanyang University, Ansan, Korea 426-791.

10.1021/nl0731466 CCC: $40.75
Published on Web 02/13/2008

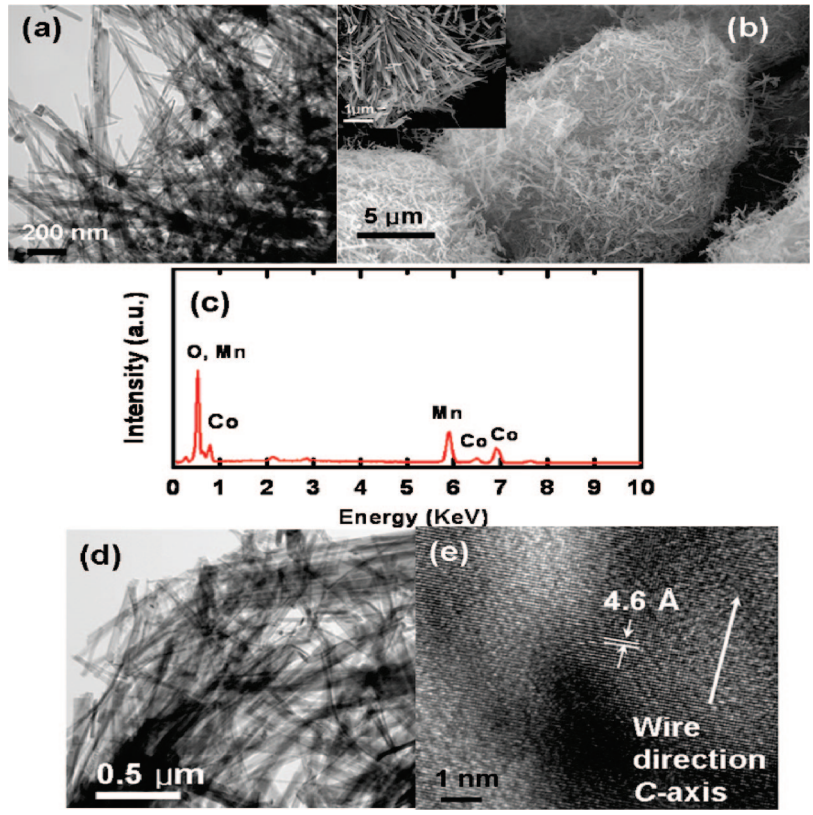

Figure 2. TEM images of (a) $Co_{0.4}Mn_{0.6}O_2$ nanowires and (b,d) SEM and TEM images of the $Li_{0.88}[Li_{0.18}Co_{0.33}Mn_{0.49}]O_2$ nanowires, respectively. Inset of (b) is an expanded image of (b). (c) Corresponding EDS spectrum of (b), and (e) high-resolution TEM image of a single nanowire of (d).

Figure 1a shows an XRD pattern of the as-prepared $Co_{0.4}Mn_{0.6}O_2$ and $Li_{0.88}[Li_{0.18}Co_{0.33}Mn_{0.49}]O_2$. The XRD pattern of the $Co_{0.40}Mn_{0.60}O_2$ is dominated by two major peaks at about 12° (110) and about 25° (200) scattering angles, which is similar to that of previously reported $Ni_{0.45}Mn_{0.55}O_2$ obtained from K-birnissite.[25] After a reaction with Li at 200 °C, the $Li_{0.88}[Li_{0.18}Co_{0.33}Mn_{0.49}]O_2$ sample clearly shows the formation of a hexagonal layered structure with a $R\bar{3}m$ space group. The lattice constants of a and c were estimated as 2.834 and 14.208 Å, respectively. Very weak superlattice reflections at approximately 20° and 24° are known to correspond to the ordering of the Li and Co and Mn ions in transition metal sites of the layered lattice.[18,19] Moreover, preferred orientation along the (003) plane was observed. The ICP-MS results showed the formation of $Li_{1.3}Co_{0.4}Mn_{0.6}O_{4.9}$; when normalized to the $LiMnO_2$, the compound had a formula $Li_{0.88}[Li_{0.18}Co_{0.33}Mn_{0.49}]O_2$.

Figure 2 shows SEM and TEM images of the as-prepared $Co_{0.4}Mn_{0.6}O_2$ nanowires (a) and $Li_{0.88}[Li_{0.18}Co_{0.33}Mn_{0.49}]O_2$ nanowires (parts b, d, and e), and $Co_{0.4}Mn_{0.6}O_2$ nanowires have a diameter of 40 nm and are >1 μm in length. After reaction with the Li nitrate, the dimension of the nanowires increases. The $Li_{0.88}[Li_{0.18}Co_{0.33}Mn_{0.49}]O_2$ nanowires have a diameter of 100 nm and a length of >3 μm. The inset of Figure 2 is an enlarged image of the edge parts of the nanowires, confirming that the particles consisted of aggregated individual nanowires.

Energy-dispersive X-ray spectrometry (EDS) of the $Li_{0.88}[Li_{0.18}Co_{0.33}Mn_{0.49}]O_2$ nanowires shows both the presence of Co and Mn. The ICP-MS results confirmed stoichiometry of $Li_{0.88}[Li_{0.18}Co_{0.33}Mn_{0.49}]O_2$. TEM image Figure 2d shows that the diameter of the nanowires is about 50 nm. The HREM image of the nanowires (image e of Figure 2) clearly shows the formation of the layered structure with the lattice fringe of the (003) plane corresponding to 0.46 nm. In addition, a number of abnormally grown nanowires that have diameters of 50 nm and lengths of >10 μm can be observed. These nanowires also comprise the layered hexagonal structure (see Supporting Information). The Brunauer–Emmett–Teller (BET) surface area of the $Li_{0.88}[Li_{0.18}Co_{0.33}Mn_{0.49}]O_2$ nanowires was 50 m^2/g.

Figure 3 shows the charge and discharge curves between 4.8 and 2 V at rates of 0.2, 1, 3, 5, 10, and 15 C (1C = 240 mA/g), corresponding to capacities of 245, 242, 238, 230, 225, and 220 mAh/g, respectively (charge rate was fixed at 1C). In general, the loading level of the active cathode material critically affects the performance of the cathode. In this case, a cathode material loading level of 20 mg/cm^2 was used (thickness of the electrode except for Al current collector was 20 μm). Note that amounts of carbon blacks and binder also affect the electrode performance and increased amount of carbon blacks improves the electrode performance but decreases the electrode density of the cell. In our case, we used 5 wt% carbon blacks and 5 wt % binder, which means 90 wt % active material was used. On the other

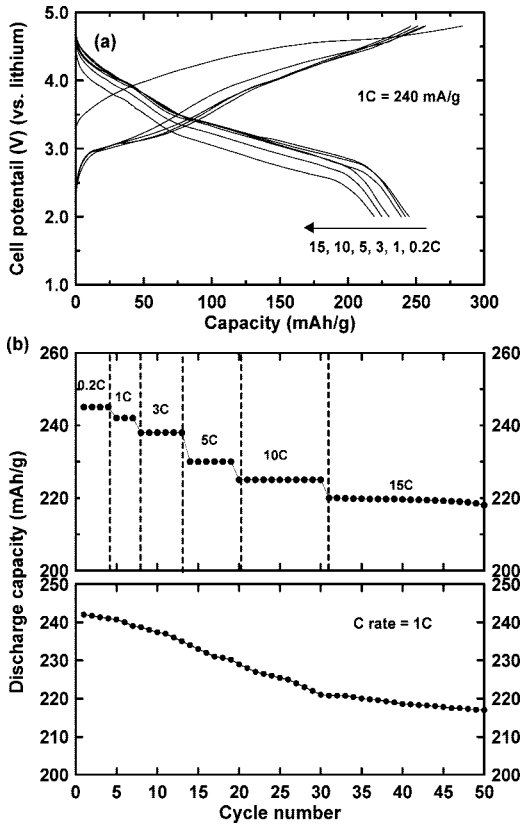

Figure 3. (a) Voltage curves of $Li_{0.88}[Li_{0.18}Co_{0.33}Mn_{0.49}]O_2$ nanowires in a coin-type half-cell at different C rates of 0.2, 1, 3, 5, 10, and 15C (1C = 240 mA/g) between 2 and 4.8 V. The charge rate was fixed at 1C, and the discharge capacities vs cycle number were tested at different C rates. (b) Discharge capacity vs cycle number of the $Li[Li_{0.08}Co_{0.33}Mn_{0.5}]O_2$ nanowires in a coin-type half-cell at a 1C rate between 2 and 4.8 V.

hand, other overlithiated $Li[Co_xLi_{1/3-x/3}M_{2-x2/3}]O_2$ (M = transition metal) compounds[24,30] used 12 wt % carbon blacks and 8 wt % binder, which means 80 wt % active material.

After the first charge process, the plateau vanished in the subsequent cycles. Although a similar irreversible voltage plateau during the first charge process has been reported with Li_2MnO_3-based oxides, Li_2MnO_3-based oxides showed a distinct flat plateau region at ~4.5 V.[30] In contrast to this, $Li_{0.88}[Li_{0.18}Co_{0.33}Mn_{0.49}]O_2$ has a inclined plateau at ~4.6 V. Presence of the inclined plateau at 4.5 V (as shown in Figure 3a) instead of the flat plateau in $Li_{0.88}[Li_{0.18}Co_{0.33}Mn_{0.49}]O_2$ nanowires is also observed in $Li[Co_xLi_{1/3-x/3}Mn_{2-x2/3}]O_2$ and $Li[Cr_xLi_{1/3-x/3}Mn_{2-x2/3}]O_2$, in which the flat plateau turn into a inclined plateau with increasing Co or Cr contents.[21,20] This is because more transition metal (Co, Cr) is available to be involved in the redox reaction, and oxygen loss should not be required for samples with higher transition metal content to remove all the Li from the Li layer.[21]

On the other hand, Dahn et al. proposed that the origin of the 4.5 V flat plateau in $Li[M_xLi_{1/3-x/3}Mn_{2-x2/3}]O_2$ with $x < {}^1/_3$ corresponded to the removal of the remaining lithium from the lithium layer along with the simultaneous ejection of oxygen.[21] Hong et al. had proposed that the long 4.5 V plateau in $Li[Ni_xLi_{1/3-x/3}Mn_{2-x2/3}]O_2$ ($x < 0.3$) could be explained in relation to a molecular orbital (MO) coming from the combination of metal d orbitals and a ligand-group orbital, originating from six oxygen orbitals.[24] According to a qualitative diagram for MO, if the oxygens have filled t_{2g} orbitals whose energies are close to those of partially filled Mn^{4+} t_{2g} orbitals, then π bonding due to oxygen → metal donation can occur. In this case, three d electrons of Mn^{4+} go into the antibonding t_{2g}^* orbitals. In this respect, these π bonding electrons due to oxygen → metal may contribute to the 4.5 V plateau. However, Bruce et al. proposed similar 4.5 V plateau origin to Dahn et al. and O_2 was evolved from such Mn^{4+}-containing compounds, $Li[Ni_{0.2}Li_{0.2}Mn_{0.6}]O_2$, on charging using in situ differential electrochemical mass spectrometry (DEMS) and powder neutron diffraction.[17] In addition, they reported that O loss from the surface is accompanied by diffusion of transition metal ions from surface to bulk, where they occupy vacancies created by Li removal.

During the first cycle, the charge and discharge capacities are 283 and 245 mAh/g, respectively, showing 87% Coulombic efficiency. After 50 cycles at a rate of 1C, capacity retention was 92%. In particular, the capacity retention at a 15C rate was 90%, compared to that at a 0.2C rate. The capacity retention of the nanowires even after repetitive cycling at a 15C rate was 98%. The rate capability of the cathode with the irregularly distributed particles was determined by the larger particles, and therefore it is hampered by the larger particles with longer Li ion diffusion distance. For instance, $Li[Ni_{0.20}Li_{0.2}Mn_{0.6}]O_2$ nanoparticles with the primary particles were narrowly distributed in the range of 80–200 nm, and with large aggregates of 1–20 μm[24] showed the first discharge capacity of ~280 mAh/g at 20 mA/g, but its discharge capacity significantly decreased to 210 mAh/g at 400 mA/g. However, our nanowire has a uniform diameter of about 50 nm and shows first discharge capacity of 245 mAh/g at 48 mA/g and its capacity is 220 mAh/g at 3000 mA/g. The capacity retention of the $Li[Ni_{0.41}Li_{0.08}Mn_{0.51}]O_2$ nanoparticle with 20–200 nm sizes (BET surface area was 24 m^2/g) at a current rate of 1200 mA/g rate is 89%, while that of the nanowire is 94% at the same current. Even though 6% difference is small at lower current rates, higher current rates can make a huge difference. Accordingly, the capacity retention of the nanowires is expected to be much higher than that of the nanoparticles at higher current rate than 1200 mA/g. This indicates that the nanowires with higher surface areas likely lead to higher electrode/electrolyte contact areas. This coupled with shorter diffusion paths into the lattices and reduced strain of intercalation may lead to improved cycling performance compared to nanoparticles.

Figure 4 shows the normalized Mn and Co K-edge XANES (X-ray absorption near edge structure) features for a pristine cathode sample (before charging) as well as the same sample after 50 cycles, compared with references with different oxidation states ($LiNi_{1/3}Co_{1/3}Mn_{1/3}O_2$, $LiMn_2O_4$ spinel, $LiCoO_2$). All of the Mn K-edge XANES spectra show doubly split pre-edge peaks, denoted by A1 and A2; these are assigned as quadruple-allowed 1s → 3d (e_g) and 1s → 3d (t_{2g}) transitions, respectively. An intermediate bump exists

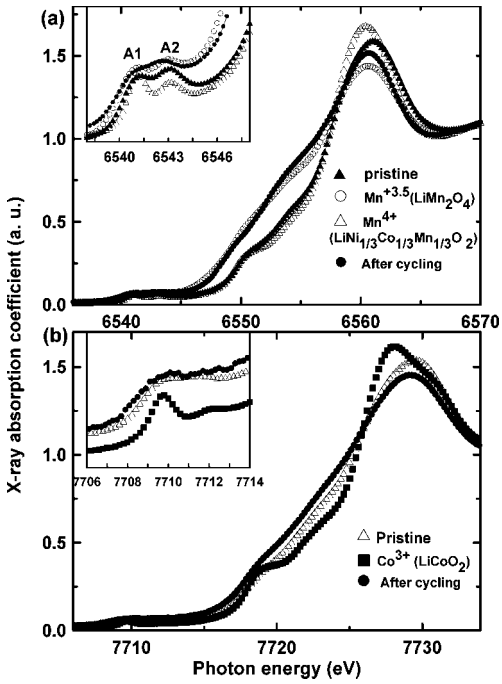

Figure 4. (a,b) Mn and Co K-edge XANES (X-ray absorption near edge spectra) of $Li_{0.88}[Li_{0.18}Co_{0.33}Mn_{0.49}]O_2$ nanowires before and after cycling, and other references.

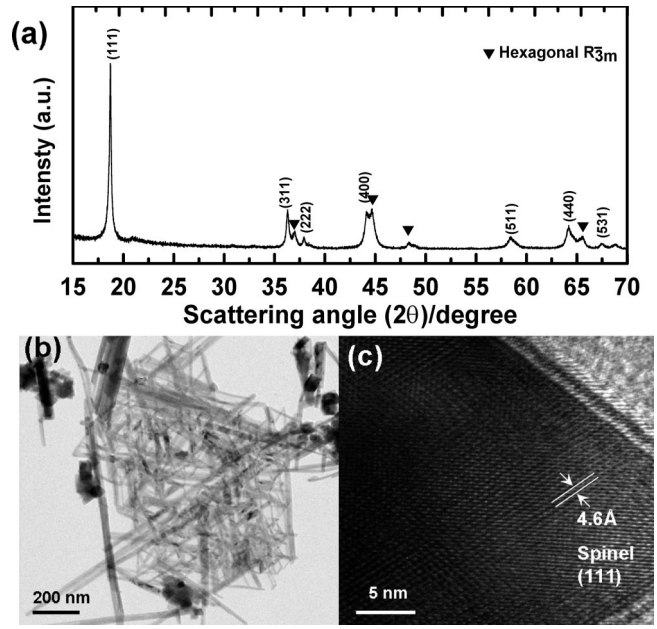

Figure 5. (a) XRD pattern of the $Li_{0.88}[Li_{0.18}Co_{0.33}Mn_{0.49}]O_2$ nanowires after 50 cycles at a 1C rate; (b,c) low- and high-magnification TEM images of (a), respectively.

at 6552 eV, of which the magnitude is related to the connectivity between the MnO_6 octahedra in the structure. This is very prominent in the pristine sample. However, such a bump completely disappeared after 50 cycles, suggesting that the connectivity between the MnO_6 octahedra in the structure was destroyed during cycling. The spectrum measured after 50 cycles shows a slight negative shift compared to that of the pristine state. This suggests that the Mn oxidation state decreases to less than 4+ and resembles the spectrum of the $LiMn_2O_4$ ($Mn^{3.5+}$). The pre-edge peak intensity (peak A2) after cycling is smaller than that of the pristine sample and is similar to that of $LiMn_2O_4$, indicating Mn oxidation state is about +3.5 after cycling. A similar negative peak shift of the Co K-edge XANES after cycling can be observed in Figure 4b, indicating that the oxidation state of the pristine sample (3+) is reduced to less than 3+ after cycling. Because the lack of Jahn–Teller distortion in the $Li[Co_xLi_{1/3-x/3}M_{2-x2/3}]O_2$ (M = transition metal) compounds during cycling is expected because the Jahn–Teller active Mn^{3+} ion is not present. However, Mn K-edge XANES spectra of $Li[Co_xLi_{1/3-x/3}Mn_{2-x2/3}]O_2$ showed spinel-like phase transition of the cathode after 20 cycles. Robertson et al. reported that Li_2MnO_3, which has no Jahn–Teller active Mn^{3+} ion, converted to spinel-like phase on cycling.[31] Conversely, in similar solid solutions of $Li[Ni_xLi_{1/3-x/3}Mn_{2-x2/3}]O_2$, there was no phase transformation nor decrease of Mn oxidation state after 20 cycles.[24]A similar result to this was reported by Bruce et al., and they reported that $Li[Li_{0.2}Ni_{0.2}Mn_{0.6}]O_2$ did not exhibit spinel-like phase transition phase after 50 cycles.[17] The difference of the cycling mechanism between $Li[Co_xLi_{1/3-x/3}M_{2-x2/3}]O_2$ and $Li[Co_xLi_{1/3-x/3}Mn_{2-x2/3}]O_2$ are still unknown.

These results are consistent with the XRD pattern and TEM image of the cycled cathode, which showed the formation of a spinel phase (Figure 5). The XRD pattern of the cycled electrode showed dominant transition into the spinel phase (*Fd3m*) with minor presence of original layered phase. Even after cycling, nanowire morphology was maintained, but an HREM image of (b) clearly showed the formation of the lattice fringe of the (111) plane of the spinel *Fd3m*, corresponding to 4.6 Å.

In conclusion, $Li_{0.88}[Li_{0.18}Co_{0.33}Mn_{0.49}]O_2$ nanowires were directly prepared via a hydrothermal reaction at 200 °C. The cathode nanowires showed a high reversible capacity corresponding to 230 mAh/g at a 1C rate and showing excellent capacity retention with rate cycling as high as 15C.

Acknowledgment. This work was supported by the IT R&D program of MIC/IITA (2006-S-057-01, 4.35V Cathode Material for Cellular Phone Power Source). We acknowledge the Pohang Light Source (PLS) for the XAS measurement.

Supporting Information Available: Experimental section and SEM image/EDS and TEM images of the abnormally grown nanowires. This material is available free of charge via the Internet at http://pubs.acs.org.

References

(1) Peng, X.; Manna, L.; Yang, W.; Wickham, J.; Scher, E.; Kadavanich, A. *Nature* **2000**, *404*, 59.
(2) Jun, Y.; Lee, S.-M.; Kang, N.-J.; Cheon, J. *J. Am. Chem. Soc.* **2001**, *123*, 5150.
(3) Manna, L.; Scher, E. C.; Alivisatos, A. P. *J. Am. Chem. Soc.* **2000**, *122*, 12700.
(4) Jun, Y.-W.; Choi, J.-S.; Cheon, J. *Angew. Chem., Int. Ed.* **2006**, *45*, 3414.
(5) Wang, Y.; Lee, J. Y.; Deivaraj, T. C. *J. Phys. Chem. B* **2004**, *10*, 13589.
(6) Wang, Y.; Lee, J. Y.; Zeng, H. C. *Chem. Mater.* **2005**, *17*, 3899.
(7) Wang, Y.; Zeng, H. C.; Lee, J. Y. *Adv. Mater.* **2006**, *18*, 645.
(8) Zhao, Z. W.; Guo, Z. P.; Wexler, D.; Ma, Z. F.; Wu, Z.; Liu, H. K. *Electrochem. Commun.* **2007**, *9*, 697.

(9) Armstrong, G.; Armstrong, A. R.; Canales, J.; Bruce, P. G. *Electrochem. Solid State Lett.* **2006**, *9*, A139.
(10) Gao, X. P.; Lan, Y.; Zhu, H. Y.; Liu, J. W.; Ge, Y. P.; Wu, F.; Song, D. Y. *Electrochem. Solid State Lett.* **2005**, *8*, A26.
(11) Wang, Q.; Wen, Z.; Li, J. *Inorg. Chem.* **2006**, *45*, 6944.
(12) Armstrong, A. R.; Armstrong, G.; Canales, J.; Bruce, P. G. *Angew. Chem., Int. Ed.* **2004**, *43*, 2286.
(13) Hu, Y.-S.; Kienle, L.; Guo, Y.-G.; Maier, J. *Adv. Mater.* **2006**, *18*, 1421.
(14) Armstrong, A. R.; Armstrong, G.; Canales, J.; Garcia, R.; Bruce, P. G. *Adv. Mater.* **2005**, *17*, 862.
(15) Park, D. H.; Lim, S. T.; Hwang, S.-J.; Yoon, C.-S.; Sun, Y.-K.; Choy, J.-H. *Adv. Mater.* **2005**, *17*, 2834.
(16) Lu, Z.; Dahn, J. R. *J. Electrochem. Soc.* **2002**, *149*, A815.
(17) Armstrong, A. R.; Holzapfel, M.; Novak, P.; Johnson, C. S.; Kang, S.-H.; Thackeray, M. M.; Bruce, P. G. *J. Am. Chem. Soc.* **2006**, *128*, 8694.
(18) Park, S.-H.; Kang, S.-H.; Johnson, C. S.; Amine, K.; Thackeray, M. M. *Electrochem. Commun.* **2007**, *9*, 262.
(19) Thackeray, M. M.; Johnson, C. S.; Vaughey, J. T.; Li, N.; Hackney, S. A. *J. Mater. Chem.* **2005**, *15*, 2257.
(20) Johnson, C. S.; Li, N.; Lefief, C.; Thackeray, M. M. *Electrochem. Commun.* **2007**, *9*, 787.
(21) Lu, Z.; Dahn, J. R. *J. Electrochem. Soc.* **2002**, *149*, A1454.
(22) Ammundsen, B.; Paulsen, J. *Adv. Mater.* **2001**, *13*, 943.
(23) Hong, Y.-S.; Park, Y. J.; Wu, X.; Ryu, K. S.; Chang, S. H. *Electrochem. Solid State Lett.* **2003**, *6*, A166.
(24) Hong, Y.-S.; Park, Y. J.; Ryu, K. S.; Chang, S. H.; Kim, M. G. *J. Mater. Chem.* **2004**, *14*, 1424.
(25) Cho, J.; Kim, Y.; Kim, M. G. *J. Phys. Chem. C* **2007**, *111*, 1186.
(26) Ching, S.; Landrigan, J. A.; Jorgensen, M. L. *Chem. Mater.* **1995**, *7*, 1604.
(27) Le Goff, P.; Baffier, N.; Bach, S.; Perei-Ramos, J. P. *Mater. Res. Bull.* **1996**, *31*, 63.
(28) Ching, S.; Petrovay, D. J.; Jorgensen, M. L.; Suib, S. L. *Inorg. Chem.* **1997**, *36*, 883.
(29) Xu, Y.; Feng, Q.; Kajiyoshi, K.; Yanagisawa, K.; Yang, X.; Makita, Y.; Kasaishi, S.; Ooi, K. *Chem. Mater.* **2002**, *14*, 3844.
(30) Park, Y. J.; Hong, Y.-S.; Wu, X.; Kim, M. G.; Ryu, K. S.; Chang, S. H. *J. Electrochem. Soc.* **2004**, *151*, A720.
(31) Robertson, A. D.; Bruce, P. G. *Chem. Commun.* **2002**, 2790.

NL0731466